# The National Bureau of Standards primary high-vacuum standard

C. R. Tilford, S. Dittmann, and K. E. McCulloh
*National Bureau of Standards, Center for Basic Standards, Gaithersburg, Maryland 20899*

(Received 8 February 1988; accepted 3 May 1988)

The theory, design, operating procedures, and estimated errors are discussed for an orifice-flow-type pressure standard currently in use at the National Bureau of Standards. This standard is used to define pressures between $10^{-7}$ and $10^{-1}$ Pa. Including the uncertainty of the flowmeter, the estimated total uncertainty varies from 2.6% at the highest pressures, to 1.4% at midrange, and 8.2% at the lowest pressures. Representative calibration results are presented for four different types of hot-cathode ionization gauges.

## I. INTRODUCTION

At pressures below $\sim 10^{-1}$ Pa ($10^{-3}$ Torr) (1 Torr = 133.322 Pa) the flow of gas through an orifice of known area can be used as a primary pressure standard. The National Bureau of Standards (NBS) has used this dynamic or orifice-flow technique to develop a standard that is used routinely between $10^{-1}$ and $10^{-6}$ Pa and on an exploratory basis to lower pressures. An early version of this system is described in Ref. 1, and a brief description of the present system is given in Ref. 2. This paper will briefly develop the theory of this standard, describe the design of the vacuum chamber, including the orifice, and evaluate the performance of the pressure standard. The flowmeter that is an integral part of this standard is discussed in a separate publication.[3]

## II. THEORY OF ORIFICE-FLOW STANDARDS

Orifice-flow standards have been discussed in recent reviews.[4,5] Generally the theory of these devices is described in terms of "throughput" and conductance (generally designated $Q$ and $C$). In order to avoid ambiguities in the definition of certain flow units[6] the present description will be in terms of more fundamental quantities, but the results are completely equivalent.

From the kinetic theory of gases, the pressure due to molecules of a single gas species incident at a surface is given by

$$P = (2\pi kTm)^{1/2}F, \tag{1}$$

where $k$ is Boltzmann's constant, $T$ is the molecular temperature, $m$ is the molecular mass, and $F$ is the molecular flux incident on unit area. The pressure due to a multispecies mixture will be a linear sum of such contributions.

If a molecular flow rate $\dot{n}$ (molecules/s) is admitted to a chamber pumped by a "perfect" pump through an orifice of area $A$, under conditions of constant pressure and molecular flow (molecule–molecule collisions are a negligible fraction of the molecule–wall collisions), the flux incident at the orifice will be given by $\dot{n}/A$ and the pressure at the orifice is

$$P = (2\pi kTm)^{1/2}\dot{n}/A\,. \tag{2}$$

If $A$ is a small fraction of the chamber surface area, and the inlet flow is baffled so that molecules must make several collisions with the chamber walls before being pumped out, the pressure will approach uniformity throughout the chamber and $T$ will be very close to the average chamber wall temperature. Thus, knowing $A$ and using a flowmeter to measure $\dot{n}$, the pressure in the chamber could be calculated. However, two important modifications must be made to Eq. (2) to account for deviations from ideal conditions.

Equating the incident flux to the flow rate divided by the area of the orifice is strictly true only in the case of an orifice with zero thickness. Molecular scattering from the edges of a real orifice or nearby structures in a line of sight from the orifice will perturb the flux at the orifice. This can be taken into account by calculating an effective area $A_e$ using the transmission probability approach of Clausing.[7]

A second complication is that perfect pumps are generally not available and usually there is a significant return flux coming back into the chamber through the orifice. Under conditions of constant pressure in the calibration chamber, this return flux is balanced by a corresponding flux back out through the orifice, and the flow rate from the flowmeter into the chamber $\dot{n}$ equals the net flow out through the orifice. The "high" pressure in the chamber $P_H$ is related by Eq. (1) to the total flux out through the orifice, which is the net flux $\dot{n}/A_e$ plus the return flux. The return flux can be calculated from the "low" pressure $P_L$ on the downstream side of the orifice using Eq. (1). Thus, the pressure difference across the orifice can be calculated knowing the net flow through the chamber and the effective area of the orifice:

$$P_H - P_L = (2\pi kTm)^{1/2}\dot{n}/A_e\,. \tag{3}$$

A method of correcting for $P_L$, allowing the calculation of $P_H$, will be described in a later section.

## III. DESCRIPTION OF EQUIPMENT

### A. Vacuum chamber

The design of the vacuum chamber, illustrated in Fig. 1, is largely determined by the need to maintain a low background pressure, to provide room to mount the gauges to be calibrated, and to maintain a geometry for which the orifice conductance calculations will be valid and adequate pressure uniformity can be assured. The chamber is in two cylindrical halves, each 27 cm in diameter and 34 cm long, separated by a central wall with the orifice in the center. A chamber of this size permits the incorporation of eight $2\frac{3}{4}$-in.-o.d. (3.5-cm-i.d.) gauge mounting flanges on the upper half at a circumference 13.3 cm above the orifice. A circular baf-

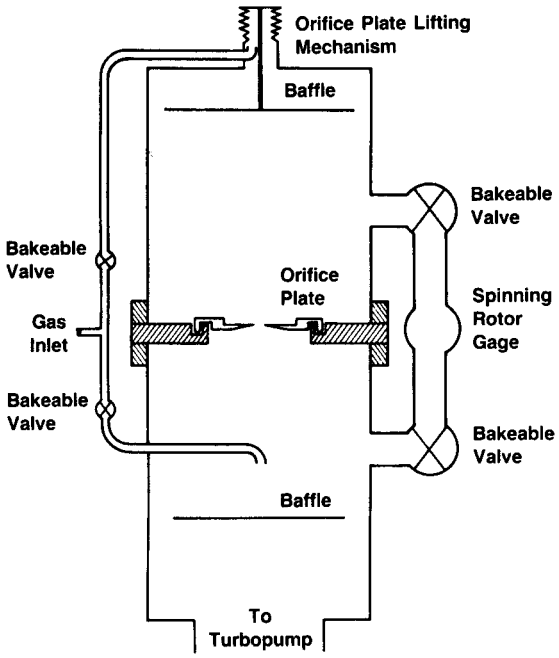


FIG. 1. Schematic of the vacuum chamber. Only one of the eight gauge mounting ports available on each chamber half is shown. A residual gas analyzer mounted in the calibration chamber (not shown) is used to monitor base vacuum conditions and calibration gas purity. The gas inlet is connected to the flowmeters by baked stainless-steel lines.

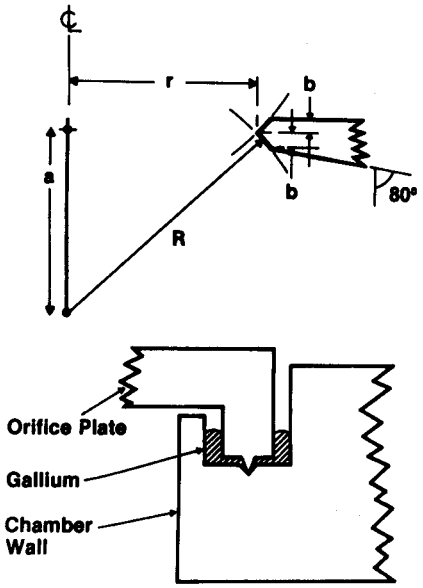


FIG. 2. Detail of the orifice and the gallium-filled groove that seals the orifice plate into the wall between the two chamber halves. In order to obtain a continuous band of gallium around the groove a stainless-steel rod was used to "scrub" or "scratch" the bottom of the groove after filling with the gallium. The lip of the orifice plate was thoroughly passivated.

fle 5 cm below the top of the upper chamber insures that gas molecules entering the top of the upper chamber from the flowmeter will experience several collisions with the chamber walls before entering a gauge or passing through the orifice at the bottom. These collisions are essential to insure the random distribution of molecular velocities, which is necessary for pressure uniformity and is assumed in the conductance calculation. As discussed below, the uniform distribution of molecular flux will be perturbed by the molecules entering the chamber below the baffle and by those escaping through the orifice. This perturbation can be kept within acceptable bounds by using an orifice whose area is a small fraction of the surface area of the chamber. At the same time, the orifice conductance must be large enough to maintain a low background pressure and ensure a high enough flow that gauge pumping and outgassing are minor perturbations. In our system the compromise used is a nominal 1.1-cm-diam orifice, described in detail below, with a nitrogen pumping speed at 23 °C of $\sim 11\,700$ cm$^3$/s, and an area that is 0.03% of the upstream chamber area.

Accounting for the molecules returning back through the orifice into the calibration chamber will be most accurately done if these molecules originate from a uniform flux distribution. This is achieved by making the lower chamber an almost symmetric duplicate of the upper chamber, with a baffle 12 cm above the inlet of the nominal 0.5 m$^3$/s turbomolecular pump attached to the bottom of the chamber. The chamber is not perfectly symmetrical as the baffle is located 24 cm below the orifice. The effective rate of exhaust from the lower chamber is 0.3 m$^3$/s for nitrogen. The turbomolecular pump was chosen for its stable high pumping speed, low base pressure, and compatibility with most gases.

Ultrahigh vacuum construction practices are employed throughout; the chamber is stainless steel, only metal seals are used, and the chamber and all gauges are baked between 200 and 250 °C after each venting to air. However, the small orifice clearly would restrict the attainment of a low base pressure in the upper chamber. Therefore, the orifice is contained in a plate that seals into a gallium-filled groove, located in the central wall as illustrated in Figs. 1 and 2. During pumpdown or bakeout, the orifice plate can be lifted through a bellows at the top of the chamber, opening a 12.7-cm hole between the upper and lower chambers. For the gallium to form a seal when the orifice plate is lowered back down, it must remain supercooled for prolonged periods below its 29.8 °C melting temperature, a well-known characteristic of gallium. Leaks of 10 cm$^3$/s or larger will have a significant effect on our measurements. In four years of operation we have never observed any evidence of seal failure. Nor have we seen any evidence of gallium vapor in the chamber, which is consistent with the prediction that gallium's room-temperature vapor pressure will be many decades below the detection limit of any vacuum sensor.

When the several meters of $\frac{3}{8}$-in.-o.d. (0.95-cm) stainless-steel line connecting the standard to the flowmeters are baked along with the chamber, this system routinely attains base pressures in the low $10^{-8}$ Pa ($10^{-10}$ Torr) range, the residual gas is almost entirely hydrogen. The base pressure in the calibration chamber typically will increase on the order of a factor of 2 when the orifice plate is lowered and sealed in the gallium groove, although increases as large as a factor of 6 have been observed with 17 hot cathode ion gauges and gas analyzers operating in the calibration chamber. In this latter case a day was required after the

orifice plate was lowered for the rate of change of pressure to become $<0.3\%/\text{h}$.

### B. Orifice

The orifice proper, as shown in Fig. 2, is a sharp-edged hole at the center of a 15.2-cm-diam stainless-steel plate. The outer edge of the plate includes the lip that fits into the gallium-filled groove in the wall between the chamber halves. A 1.12-cm-diam hole was bored through the center of the plate where it is 0.74 mm thick. The orifice was formed by lapping the hole with a steel ball of 1.587-cm (0.6250-in.) diameter to nominally equal depths from above and below. This technique was chosen because of the ease of calculating transmission probabilities for the spherical surfaces, and the expectation that it would result in a clean edge. Upon final lapping with an unworn ball, the two concave spherical surfaces thus generated met at a sharp circular edge with a measured diameter of $1.1240 \pm 0.0008$ cm and a computed edge angle of 90.1°. Microscopic examination revealed smooth surfaces and a sharp, burr-free edge. Above the orifice the orifice plate is flat out to a diameter of 8.89 cm, where there is a 0.61-cm step. On the bottom side there is a truncated 80° half-angle cone. Effective area correction factors are calculated for both of these features.

### C. Area calculation

Calculation of the orifice effective area, carried out by McCulloh,[8] is based on the molecular transmission probability approach initiated by Clausing.[7] It assumes free molecular flow and cosine law scattering at surfaces. The area is given by

$$A_e = \pi r^2 K_0 K_1 K_2, \tag{4}$$

where $r$ is the measured radius of the lapped hole, $K_0$ is the transmission probability of the duct formed by the lapped spherical surfaces, $K_1$ is the transmission probability of the 8.89-cm-diam cylindrical relief in the top of the orifice plate, and $K_2$ is the transmission probability of the 80° cone in the bottom of the plate.

Estimates based on a generalization of Clausing's theory for cylindrical geometries place bounds on $K_1$ of

$$0.999\,95 < K_1 < 0.999\,97.$$

The results of Iczkowski *et al.*[9] were used to place bounds on $K_2$ of

$$0.9999 \leqslant K_2 < 1.0000.$$

This gives us a mean value for the product $K_1K_2 = 0.9999$, with a maximum error of $7\times10^{-5}$.

The calculation of $K_0$ involves an integral equation that yields the result

$$K_0 = 1 - 2J/(R + a), \tag{5}$$

where $R$ is the radius of curvature of the lapped spherical surfaces, $a$ is the distance from the center of curvature to the center of the orifice, and $J$ is an integral over the surface of the orifice duct of the probability that a molecule striking that surface will not pass into the lower chamber. This integral has not been evaluated exactly, but it is within the limits

$$0.147\,92b < J < 0.148\,01b,$$

where $b$ is the half-thickness of the orifice duct. Using the appropriate dimensions in Eq. (5) we then have

$$0.991\,672 < K_0 < 0.991\,677.$$

These bounds are uncertain by 0.03% due to the uncertainty of the measured quantities used.

Combining the above we find that at 23 °C

$$A_e = 0.9916\pi r^2 = 0.9838 \text{ cm}^2. \tag{6}$$

The overall uncertainty is $\pm$ 0.18%, with the largest contribution being 0.14% due to the uncertainty in the measured value of $r$.

## IV. CALCULATION OF ABSOLUTE PRESSURES

In the system described here the pressure downstream of the orifice is ~3.7% of the pressure in the calibration chamber for nitrogen. The ratio of these pressures varies, to the first order, with the inverse of the square root of the molecular mass. It is difficult to measure $P_L$ directly since this would require a gauge calibrated below the range of pressure generated by the standard. However, if we can measure the ratio of the pressures upstream $P_H$, and downstream $P_L$, from the orifice,

$$R_p = P_H/P_L, \tag{7}$$

then

$$\begin{aligned} P_H &= (P_H - P_L)[R_p/(R_p - 1)] \\ &= (2\pi kTm)^{1/2}(\dot{n}/A_c)[R_p/(R_p - 1)]. \end{aligned} \tag{8}$$

The pressure ratio $R_p$ is measured by a molecular drag gauge [10](MDG) that, as shown in Fig. 1, can be connected through $1\frac{1}{2}$-in. (3.8-cm) bakable valves to one of the gauge ports in the upper chamber or to a similar port in the lower chamber. Since the MDG is inert and therefore not limited by plumbing impedances, and reproducible at the 1% or better level above $10^{-4}$ Pa, it can be used to determine $R_p$ quite precisely in the high-vacuum range. This is done during each calibration cycle. Errors in $R_p$, whether random or due to the systematic pressure gradients discussed below, will be reduced in effect on the generated pressure by the factor $1/(R_p - 1)$, which is ~0.04 for nitrogen. A more significant problem is that as the pressure is reduced, the random error of the MDG, typically $10^{-6}$ Pa or greater, precludes its use for a direct determination of $R_p$. $R_p$ will be a function only of the orifice conductance and the pump speed, and in the molecular flow range the only variable with pressure can be the turbomolecular pump speed. As detailed below, we have indirectly found the pump speed, and therefore $R_p$, to be constant to within several percent down to a lower chamber pressure of $3\times10^{-8}$ Pa. $R_p$ will also be sensitive to any leakage through the gallium seal. Apart from changes associated with a failing turbomolecular pump bearing we have not seen significant changes with time of $R_p$, indicating reliable operation of the gallium seal.

## V. EXTENSION TO LOWER PRESSURES

The low-pressure limit of orifice-flow standards is determined by the low flow limit of the flowmeter and by the base pressure of the vacuum chamber. In the case of the NBS system, the base pressure is below the limit established by the flowmeter. Although the system has been operated with gas flow into the calibration chamber down to $10^{-6}$ Pa, it is typically limited to pressures above $10^{-5}$ Pa in this mode in order to limit the contributions of flowmeter errors. We have extended the range of the pressure standard by injecting the gas flow into the lower pressure half of the vacuum chamber, downstream from the orifice. The pressure gradients in the lower chamber preclude the direct calculation of the resultant pressure in the calibration chamber. However, we can experimentally determine the ratio of the flows, $R_f$, into the two chambers required to generate the same pressure. A pressure $P$ is established by a measured flow from the flowmeter $\dot{n}_H$ into the calibration chamber. Using the valves shown in Fig. 1 the flowmeter is then connected to the lower chamber and the flow increased until the same pressure is established in the upper chamber. This measured flow $\dot{n}_L$ is used to derive the flow ratio

$$R_f = \dot{n}_L/\dot{n}_H. \tag{9}$$

Equation (8) is then modified to give

$$P_H = (2\pi kTm)^{1/2}(\dot{n}_L/R_f A_e)[R_p/(R_p - 1)]. \tag{10}$$

Molecular drag and ion gauges in the upper chamber are used to determine $R_f$. There is a random error in the determination of $R_f$ of the order of 0.1%. More importantly, there is an additional systematic uncertainty due to the two flowmeter measurements required. This effectively doubles the contribution of the flowmeter error in Eq. (10). In the NBS standard, $R_f$ differs from $R_p$ by $<1\%$ although this may be fortuitous since flux and pressure gradients of several percent are known to exist in the lower chamber.

The flow ratio cannot be directly measured for pressures lower than those that can be reliably generated by a measured flow into the upper chamber, so it is typically determined between $10^{-4}$ and $10^{-5}$ Pa. However, since the system is clearly in the molecular flow regime at these low pressures, both $R_f$ and $R_p$ will be constant with decreasing pressure if the turbomolecular pump speed does not change with pressure. As noted before, we have indirect evidence that the pump speed changes very little down to $3\times10^{-8}$ Pa.

## VI. EVALUATION OF ERRORS

In addition to the errors already discussed in the conductance calculation and the measurement of the pressure and flow ratios, $R_p$ and $R_f$, several other possible sources of error must be taken into account.

### A. Pressure gradients

A high degree of pressure spatial uniformity from port to port on the calibration chamber has been demonstrated by establishing a nitrogen flow to generate a pressure of $\sim10^{-3}$ Pa in the calibration chamber. The pressure was measured by four ion gauges which were well distributed about the calibration chamber. After recording the gauge readings, the orifice plate was raised and the flow was increased by a factor of $\sim15$ to reestablish the same pressure. The relative gauge readings with the orifice plate raised agreed to within 0.1% with the reading obtained with the orifice plate lowered. Since nonuniformity due to axial asymmetry of the flow would be proportional to the flow rate required to generate a specified pressure, the results indicate that any such nonuniformity to be $<0.01\%$ in normal operation with the orifice plate lowered.

The calibration chamber pressure will have a vertical perturbation due to the net flow of molecules between the gas inlet and the orifice. This will have two contributions, one due to the molecules exiting through the orifice and not being scattered back, and the second due to the molecules entering from the inlet. The first contribution is reasonably straightforward to calculate since the orifice is a nearly ideal sink. This contribution will decrease the pressure at the gauge ports from that given in Eq. (8) by the factor $r^2/4r_c^2$, where $r$ is again the orifice radius and $r_c$ is the chamber radius. For the NBS system, this factor is 0.999 57.

The second contribution is more difficult to calculate because the scattering of the inlet flow produces a diffuse source and it will take several collisions before the effects of the initial nonuniformity are negligible. However, estimates of this contribution indicate that it is somewhat smaller than the first, but of the opposite sign.

### B. Mounting of the orifice plate

Another small error is the perturbation to the calculated conductance caused by the mounting of the orifice plate. The orifice plate is mounted in the wall between the two chambers with a short duct, 12.7 cm in diameter and 1.27 cm long, between it and the lower chamber. The transmission probability to the lower chamber of molecules exiting the orifice is estimated to be $0.9997 \pm 0.0001$. This effectively increases the pressure in the upper chamber by a factor of 1.0003, offsetting the effect at the gauge port of the small vertical pressure gradient previously discussed.

We estimate that 0.003% is a generous upper bound on the uncertainties caused by the combined upper chamber pressure gradients and the mounting configuration of the orifice plate.

### C. Temperature

The average temperature of the gas molecules is determined by the average temperature of the chamber walls, which is known with an uncertainty of 0.3 K, in the absence of heat sources, notably ion gauges. Depending on the number of gauges, and whether they are tubulated or immersed in the chamber, this uncertainty, in extreme cases, could be as much as an order of magnitude larger. This will contribute an uncertainty to the pressure varying from 0.05% to 0.5%. This does not include thermal transpiration effects for ion gauges being calibrated. These are considered a part of the gauge's calibration and can cause additional errors during

later use of the gauge if its thermal environment differs from that at the time of calibration.

### D. High-pressure nonlinearities

The calculation of the orifice conductance assumes an absence of molecule–molecule collisions. The number of such collisions increases with pressure, with a corresponding increase in the error of the conductance calculation. We have chosen at this time not to attempt to correct for this effect but rather to restrict the upper pressure limit of the standard to keep this error within bounds. This error amounts to 0.1% at $\sim 8.5\times 10^{-3}$ Pa for $N_2$ and at $\sim 2.5\times 10^{-2}$ Pa for He, and increases linearly with pressure.

### E. Flow rate errors

The systematic uncertainties of the flowmeter, detailed in Ref. 3, contribute directly to the errors of the high-vacuum standard.

### F. Observed random errors and pump speed changes

Random errors, and systematic errors due to changes in pump speed with pressure, can be evaluated from the results of vacuum gauge calibrations using the primary standard. In all cases these data can at best give an estimated upper bound to the errors of the standard since the data will include not only errors due to the standard, but also those due to short- and long-term gauge instabilities and, in some cases, systematic changes of the gauge sensitivities with pressure. At higher pressures, where molecular drag gauge calibrations repeated over a few day's time are used to estimate random errors, the contribution of gauge instabilities are probably not significant. Higher pressure ion gauge calibrations repeated over a few day's time typically show somewhat larger but still relatively small effects of gauge instability. However, in the case of ion gauge data used to evaluate errors below $10^{-5}$ Pa the gauge performance probably makes a significant contribution to the observed variation of the calibration data. The amount of such data is limited, and it has been necessary to include data taken under somewhat different conditions and over periods of from one to two months. The magnitude of ion gauge instabilities varies with gauge type,[11] but some can show quite large changes operating over a month's time.[12] We have calibrated 18 gauges below $10^{-5}$ Pa, using controllers of known reliability and electrometers of known accuracy.

Examples of such data for four different types of hot-cathode ionization gauges are shown in Fig. 3. In each case the differential sensitivity or sensitivity coefficient,

$$S = (I^+ - I_0^+)/I_e(P - P_0) \qquad (11)$$

was measured, where $I_e$ is the electron emission current, $I^+$ is the collector current at pressure $P$, and $I_0^+$ is the collector current at base pressure. The primary standard determines the pressure increase, $P - P_0$, above base pressure. The fractional or percentage changes of this sensitivity from its value at low pressures are plotted as a function of pressure to a uniform scale, indicated on the figure. The nude Bayard/Alpert (B/A) gauge has two thoria coated filaments. Data are shown for one filament operated at an emission current of 1 mA. The average low-pressure nitrogen sensitivity was 0.155 $Pa^{-1}$ (20.7 $Torr^{-1}$). The peak in sensitivity between $10^{-3}$ and $10^{-2}$ Pa is quite typical of this type of gauge, although the magnitude and location of this peak may vary significantly from gauge to gauge. The modulator gauge was operated with the modulator held at grid potential. Its tungsten filament was operated at an emission current of 1 mA. Low-pressure sensitivity was 0.178 $Pa^{-1}$ (23.7 $Torr^{-1}$). The extractor gauge had an iridium filament operated at an emission current of 1.85 mA. Its low-pressure sensitivity was 0.065 $Pa^{-1}$ (8.7 $Torr^{-1}$). The glass tubulated B/A gauge has two tungsten filaments, one of which was operated at an emission current of 1 mA. Its low-pressure sensitivity was 0.078 $Pa^{-1}$ (10.5 $Torr^{-1}$). Constant sensitivity to the highest pressures tested is typical of this type of gauge.

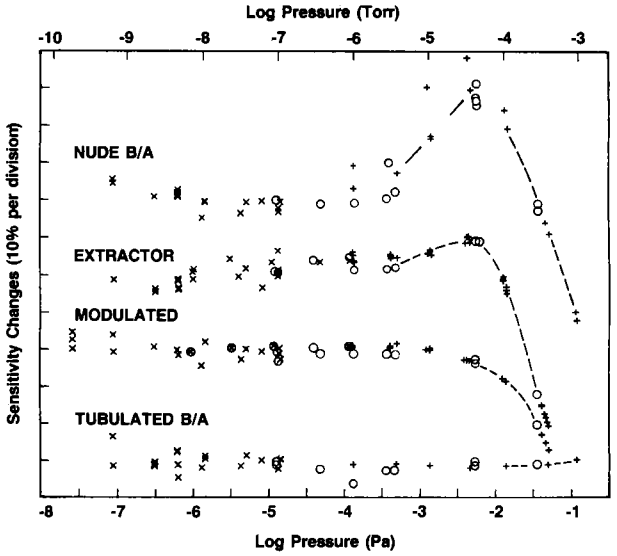


FIG. 3. Representative nitrogen calibration data for four different types of hot cathode ion gauges. Sensitivities are presented as fractional or percentage changes from the average low-pressure sensitivity for each gauge. The ×'s indicate data obtained with flow into the low pressure chamber, the O's were obtained with flow into the calibration chamber. Data obtained using molecular drag gauges, previously calibrated *in situ*, are indicated by the + 's, and are included as a reference for evaluating the repeatability of the high-pressure orifice-flow data. The dashed lines are solely to distinguish data for one gauge from another and do not represent measured or extrapolated gauge performance. The data for each gauge were acquired over a 1–2 month period.

Two of the 18 gauges showed clear evidence of instability. One changed by 8% over a four-month period, the other by 26% over the same period. Neither gauge was used for further analysis. Data for the other 16 gauges show random scatter comparable to that seen in Fig. 3. Some measure of the possible contributions from gauge instabilities can be obtained by comparing the scatter of the high-pressure data for the nude B/A to that of the modulated gauge since they were calibrated at the same time. The larger scatter in the nude B/A gauge is most likely due to instabilities in that gauge. (Note: some data points for the modulated gauge are so close as to be indistinguishable and for a few of the points data were obtained for only one gauge.) While it would be desir-

able to have data taken over shorter periods of time and under more uniform conditions, the available data still allow the best evaluation of low-pressure errors.

### 1. Random errors

A measure of the short-term repeatability at higher pressures can be obtained from repeated calibrations of six different MDG's with $N_2$ at $4.9\times10^{-3}$ Pa. In this case the calibrations were made over a period of 8 h. The pooled standard deviation of the accommodation coefficients of the six gauges was 0.026%, with no significant difference in the random errors associated with any gauge.

A more stringent measure was the repeated calibrations over several weeks of ten MDG's with argon at pressures ranging from $5\times10^{-4}$ to $3\times10^{-2}$ Pa. In this case three to five different calibration series were performed at each pressure, each series taking place on a different day and involving a complete calibration cycle, starting with the vacuum chamber and flowmeter at base vacuum and the orifice plate raised above the gallium-filled groove. The data from two of the SRG's were eliminated because of clearly excessive random errors in the gauges, apparently caused by suspension instabilities. The pooled standard deviations of the remaining eight gauges were 0.10% at $3\times10^{-2}$ Pa, 0.08% at $7\times10^{-3}$ Pa, 0.12% at $3\times10^{-3}$ Pa, and 0.41% at $5\times10^{-4}$ Pa. These are consistent with other sets of MDG data.

At the lowest pressure the above results are probably dominated by the short-term random errors of the MDG's, and MDG data at yet lower pressures will not be useful in assessing errors of the standard. Therefore, we must rely on ion gauge calibration data at lower pressures.

A measure of the low-pressure short-term repeatabilities can be obtained from three calibrations repeated over several hours of a tubulated tungsten filament Bayard–Alpert gauge. In this case separate flowmeter measurements were made for each calibration. At $2\times10^{-4}$ Pa the calibrations differed by a maximum of 0.1%, and at $2\times10^{-5}$ Pa by 0.02%.

A more realistic assessment of the random errors can be obtained from calibrations repeated on different days. For flow directly into the calibration chamber, using Eq. (8), we expect that errors at the lowest pressures will be dominated by random flowmeter errors. Typically, such calibrations repeat to within $\pm 5\times10^{-8}$ Pa.

Repeated calibrations with flow into the lower pressure chamber are available for 16 different gauges at pressures from $4\times10^{-3}$ to $3\times10^{-8}$ Pa. Most of the data are below $10^{-5}$ Pa. Calibrations repeated at the same pressure on different days for most gauges vary by $< \pm 2.5\%$, even down to the lowest pressures. Linear curves fitted as a function of pressure to the sensitivities for individual gauges had standard deviations of the residuals that varied from 0.26% to 3.25% with an average standard deviation of 1.95%. Maximum deviations of individual points from the fitted curves were as large as 7.6%, although for most gauges the maximum deviations did not exceed 3%. Considering that some gauges showed larger variations than other gauges calibrated at the same time, $\pm 2.5\%$ seems a reasonable upper bound for the possible random errors of the standard with flow into the lower chamber down to $10^{-7}$ Pa.

### 2. Changes in pump speed

As discussed earlier, the pressure and flow ratios can be reliably measured only at higher pressures and their use in Eqs. (8) and (10) at lower pressures assumes the pump speed does not change with decreasing pressure. Any change in the pump speed with pressure will cause errors in both $R_p$ and $R_f$. Errors in $R_p$ will cause relatively small errors in Eqs. (8) and (10). However, errors in $R_f$ will cause corresponding errors in the pressures calculated using Eq. (10), so stability of pump speed is important at pressures below $10^{-5}$ Pa where the system is generally operated with flow into the low-pressure chamber.

Generally, $R_f$ is determined at a pressure around $10^{-5}$ Pa and ion gauge sensitivities are determined using Eq. (8) above this pressure and Eq. (10) below. However, for a few gauges sensitivities were determined using both techniques at pressures both above and below $10^{-5}$ Pa. To within the limits imposed by ion gauge instabilities, the deviations from unity of the ratios of the two sensitivities will be a measure of the constancy with pressure of $R_f$ and the pump speed. Unfortunately, in only a few cases were sensitivities determined within a short period of time (up to five days) using the two techniques. In those cases the ratios of the sensitivities varied from 0.989 to 1.006 over the pressure range $3\times10^{-6}$–$10^{-4}$ Pa. Additional data exist where the time span between the sensitivity determinations varied from 2 to 18 months. In these cases gauge instabilities are much more of a concern. The ratio of the sensitivities in these cases varied from 0.951 to 1.015 over the pressure range $10^{-6}$–$10^{-3}$ Pa.

A less direct measure of possible changes in pump speed can be obtained by examining the constancy with pressure of measured gauge sensitivities obtained from Eq. (10). It is often assumed that ion gauge sensitivities, as defined by Eq. (11), are constant at low pressures. This may or may not be true. However, a constant measured gauge sensitivity implies that either the gauge sensitivity and pump speed are both constant, or that both change with pressure in a manner such that the changes cancel. Neither case can be proven, but it is unlikely that different gauges will have the same nonlinearities, particularly if the gauges are of different designs, so, as more gauges are found to have constant measured sensitivities, to within some bounds, the second possibility becomes increasingly unlikely, and it is more probable that pump speed is constant to within those same bounds.

As can be seen in Fig. 3, there are small trends in the low-pressure data for different gauges. The trends are clearly not the same for different gauges. In order to set bounds on these trends, and possible systematic changes in pump speed, nitrogen sensitivities for each of 16 gauges, obtained with flow into the lower chamber of the standard, have been least-squares fitted to equations of the form $S = A + B \log P$. The number of data points per gauge varied from 4 to 34, the average was 16. The data extended from $3\times10^{-8}$ to $4\times10^{-3}$ Pa; most of it was below $10^{-5}$ Pa. The $B$ coefficients for the different gauges varied from $-2.5\%$ to 3.9% per decade. Only two coefficients were larger than 2.5% per dec-

TABLE I. Percentage uncertainties of the NBS high-vacuum standard with nitrogen. These error estimates are based on gas flow into the calibration chamber above $10^{-5}$ Pa, and into the low-pressure chamber at lower pressures. Random errors at $10^{-6}$ and $10^{-7}$ Pa are included in the allowance for possible errors due to changing pump speed. Since the random and systematic errors cannot be separated in this case they have not been separately summed. The systematic uncertainties have been linearly summed in order to establish an upper bound on the uncertainty.

| | Pressure (Pa) | | | | |
|---|---|---|---|---|---|
| | $10^{-1}$ | $10^{-2}$ | $10^{-3}$–$10^{-5}$ | $10^{-6}$ | $10^{-7}$ |
| Systematic contributions | | | | | |
| Orifice conductance | 0.18 | 0.18 | 0.18 | 0.18 | 0.18 |
| Molecular scattering | 1.2 | 0.12 | ... | ... | ... |
| Flow rate | 0.82 | 0.82 | 0.82 | 2.00 | 2.02 |
| Pressure ratio | 0.04 | 0.04 | 0.04 | 0.04 | 0.04 |
| Flow ratio | ... | ... | ... | 0.90 | 0.90 |
| Assumed pump speed | ... | ... | ... | 2.5 | 5.0 |
| Temperature | 0.1 | 0.1 | 0.1 | 0.1 | 0.1 |
| Total systematic | 2.34 | 1.26 | 1.14 | ... | ... |
| Random errors (3 standard deviation) | 0.21 | 0.30 | 0.30 | ... | ... |
| Total | 2.6 | 1.6 | 1.4 | 5.7 | 8.2 |

ade and they were obtained from data sets that extended down to only $10^{-6}$ Pa. The average coefficient, obtained from the individual coefficients weighted by the inverse of their variances, is $< 1\%$ per decade.

Considering the probable significant effect of ion gauge behavior on some of these data, we believe that $\pm 2.5\%$ per decade is a conservative upper bound on possible pump speed changes below $10^{-5}$ Pa.

## VII. SUMMARY OF ERRORS

The component errors previously discussed have been summarized in Table I for different pressures. The uncertainties at the highest-pressure designated "molecular scattering" are due to the high-pressure nonlinearities in the conductance of the orifice and are assessed for nitrogen. The effects due to pressure gradients in the upper chamber and orifice mounting have been left out as they are considered to be negligible. Errors at $10^{-6}$ and $10^{-7}$ Pa have been assessed on the basis of flow into the lower chamber. The flow ratio uncertainty includes random errors and a systematic contribution for the additional flowmeter measurements needed. The uncertainty due to changes in the assumed pump speed is based on the observed bounds of systematic changes in measured ion gauge sensitivities. The uncertainty for temperature errors has been somewhat arbitrarily doubled from the minimum expected value.

The tabulated random errors are upper bounds based on repeated gauge calibrations. These include the random errors of the standard, flowmeter, and gauges. The value for $10^{-3}$ to $10^{-5}$ Pa is based on three times the short-term deviations observed in ion gauge calibrations in this range. We expect that longer term random changes, due to orifice plate sealing and flowmeter seal leakage, are probably no different from those included in the higher pressure MDG data.

## ACKNOWLEDGMENT

We appreciate the continued support of this work by the Department of Energy, Office of Fusion Energy.

[1]K. E. McCulloh, J. Vac. Sci. Technol. A **1**, 168 (1983).
[2]K. E. McCulloh, C. R. Tilford, S. D. Wood, and D. F. Martin, J. Vac. Sci. Technol. A **4**, 362 (1986).
[3]K. E. McCulloh, C. R. Tilford, C. D. Ehrlich, and F. G. Long, J. Vac. Sci. Technol. A **5**, 376 (1987).
[4]K. F. Poulter, J. Phys. E **10**, 112 (1977).
[5]C. R. Tilford, J. Vac. Sci. Technol. A **1**, 152 (1983).
[6]C. D. Ehrlich, J. Vac. Sci. Technol. A **4**, 2384 (1986).
[7]P. Clausing, Ann. Phys. **12**, 961 (1932); English translation appears in J. Vac. Sci. Technol. **8**, 636 (1971).
[8]K. E. McCulloh, "Dimensions and Conductance of the Orifice in the NBS Dynamic Expander," Technical Report to the Temperature and Pressure Division of the National Bureau of Standards, 1982.
[9]R. P. Iczkowski, J. L. Margrave, and S. M. Robinson, J. Phys. Chem. **67**, 229 (1963).
[10]J. K. Fremerey, J. Vac. Sci. Technol. A **3**, 1715 (1985).
[11]S. D. Wood and C. R. Tilford, J. Vac. Sci. Technol. A **3**, 542 (1985).
[12]K. F. Poulter and C. M. Sutton, Vacuum **31**, 147 (1981).